Advances in Bamboo Science 2 (2023) 100015

Contents lists available at ScienceDirect

Advances in Bamboo Science

journal homepage: www.journals.elsevier.com/advances-in-bamboo-science

Original article

Thermal treatment of bamboo with flame: influence on the mechanical characteristics

Marco Fabiani[a,*], Silvia Greco[b], Lando Mentrasti[c], Luisa Molari[b], Giovanni Valdrè[b]

[a] *Independent Researcher, Secondary School Teacher, Pesaro, Italy*
[b] *Alma Mater Studiorum – Università di Bologna, Italy*
[c] *Università Politecnica delle Marche, Italy*

ARTICLE INFO

Keywords:
Heat treatment of bamboo
Flame treatment
Mechanical characteristics of bamboo
Bamboo durability

ABSTRACT

The mechanical properties of bamboo are susceptible to degradation due to both physical and biological agents. Among the non-chemical treatments, we studied the influence of a short-time heat treatment, using an LPG-gas torch, on the mechanical properties of a bamboo (*Phyllostachys viridiglaucescens*) growing in Italy. The response was very encouraging as we found no significant reduction in either elastic modulus or tensile, compressive and bending strength.

Several samples were subject to tension, compression and bending tests to compare the responses of the treated and untreated culms. The average tensile elastic modulus was slightly greater for the untreated culms. The average tensile strength of the untreated culms was only slightly greater, and the differences can be assumed to be insignificant from a structural point of view. The average value of the treated culms compressive elastic modulus was slightly greater than that of the untreated ones. The compressive strength was essentially the same. The bending mechanical behaviour was barely influenced by the thermal treatment.

A microscopic investigation (optical and electron microscopy) was undertaken to investigate the possible deterioration of the bamboo microstructure due to the heat treatment. No appreciable damage was detectable in the treated material.

The proposed heat treatments can be considered as a reliable and sustainable protection practice for bamboo culms.

1. Introduction

In recent years, the planting of bamboo has been receiving more and more attention from researchers and industry because of bamboo's renewable aspects. The use of bamboo as a substitute for classical construction materials could significantly reduce the impact of the construction industry in terms of global warming (Chang et al., 2018; De Flander and Rovers, 2009; Escamilla and Habert, 2014; Kavanagh et al., 2020; Van der Lugt et al., 2006, Yu et al., 2011).

The physical and mechanical properties of bamboo are similar to those of timber, as demonstrated by several authors (Chung and Yu, 2002; Gauss et al., 2019; Kaminski et al., 2016b; Molari et al., 2020). However, unlike wood, bamboo is more susceptible to degradation due to its high content of starch, sugar and protein and low content of resin, wax, and tannin (Gauss et al., 2021). The biotic agents causing decay include beetles, termites and fungi (Kaminski et al., 2016a). Bamboo is also vulnerable to abiotic degradation, and cracks and splits in bamboo culms are very common. These weaknesses are attributable to the high hydrophilicity (Zhang et al., 2021) and the structural heterogeneity of bamboo culms (Liese, 1998). Moisture losses and gains in bamboo, together with the variable density of the fibres along the culm, produce shrinking and swelling that frequently lead to the failure of the culm. It is widely recognized that untreated bamboo has limited durability (from 1 year to 5 years) (Liese and Kohl, 2015) and that it needs appropriate treatments to improve its durability.

In professional construction practice, the protection treatments for bamboo are commonly classified as chemical or non-chemical. Recently, non-chemical treatments have received particular emphasis as they are more eco-friendly and minimize impacts on human health (Kaur et al., 2016). Among the non-chemical treatments, heat treatments have attracted increasing attention. Bamboo heat treatments consist of subjecting bamboo to high temperatures for a specific time.

* Corresponding author.
E-mail address: marcofabiani.lab@gmail.com (M. Fabiani).

https://doi.org/10.1016/j.bamboo.2023.100015
Received 26 October 2022; Received in revised form 30 December 2022; Accepted 6 January 2023

(a) (b)

Fig. 1. - Treatment procedure with a gas torch (a); treated and seasoned culms (b).

Table 1 -
Moisture content and density of the treated and untreated bamboo culms.

	Not treated			Treated		
	mean	st. dev.	CV	mean	st. dev.	CV
MC [%]	9.83	0.06	0.62 %	10.19	0.17	1.66 %
Density [kg/m^3]	79.3	56.7	8.3 %	738.0	29.0	3.9 %

Steam, oil, air, inert gas, hot water, and fire are the usual media for heat-treating bamboo. Generally, the heat treatments improve the dimensional stability and the durability of bamboo (Li et al., 2022) but, on the other hand, the increasing temperature has an adverse effect on some of the mechanical properties. During heat treatments, the concentrations of extractives and lignin increase with temperature, whilst the holocellulose content decreases. This could be the reason for the adverse effect on the mechanical properties of bamboo (Silva Brito et al., 2020). On the other hand, at relatively low temperatures, the mechanical properties may be enhanced in comparison with untreated samples. Zhang et al. (2013) treated *Phyllostachys edulis* J.Houz. (syn. *P. pubescens* Mazel ex J.Houz.) culms at a temperature between 100 and 220 °C for 1–4 h, finding that the strength decreased above 160 °C, whilst the negative effects on the modulus of elasticity started at temperatures in excess of 200 °C. Xu et al. (2019) carried out tensile and compressive tests on heat-treated laminated bamboo and demonstrated that the mechanical properties decreased gradually as the temperature of the heat process increased from 20 °C to 280 °C. Manalo and Acda (2009) studied the effects of oil treatments on three species of bamboo at 160 °C and 200 °C for 30–120 min and found that the elastic modulus was reduced by 16–22% compared with untreated samples, whilst the strength showed a marked reduction of 31–60%. Yang et al. (2016) treated *Phyllostachys edulis* culms in different media (oil, air, nitrogen) at four different temperatures (150 °C, 170 °C, 190 °C, 210 °C) for three treatment durations (1 h, 2 h, 4 h). Both the strength and the elastic modulus increased in treatments up to 170–180 °C, but decreased when the temperature was raised in excess of 190 °C. Colla et al. (2011) applied a thermal treatment process on *Dendrocalamus giganteus* Munro at several temperatures, ranging from 140 °C to 300 °C. There appeared to be an optimal range of temperature, from 140 °C to 220 °C, beyond which the treatment tended to damage the bamboo's structures.

Our study aimed to assess how the rapid high temperature heating of the culm, using a gas torch, would affect the mechanical properties of the bamboo, a traditional practice proposed here in a simplified and efficient procedure. Physical and mechanical tests were carried out according to ISO 22157 (2019) and UNI 11842 (2021) to evaluate the moisture content, density, tensile, compressive strength and bending strength of *Phyllostachys viridiglaucescens* bamboo. The tests were undertaken on both untreated and treated culms to ascertain the effects of this high temperature treatment on the bamboo material.

2. Bamboo origin and flame treatment

2.1. Culm selection

Phyllostachys viridiglaucescens was cultivated in a small bamboo nursery located in Corridonia, Macerata, Italy. Twelve culms were randomly selected: six were seasoned untreated (N), and six were treated (T) with a gas torch (Fig. 1a). From each culm, two 1 m sections were identified: the bottom part (bot), 0.5–1.5 m from the ground and the top part (top), 2.5–3.5 m from the ground.

2.2. Flame treatment

In the past, the attempts to treat the culms chemically with salts and alkali (boric acid and borax) did not give satisfactory results, because a diffuse, often severe, cracking appeared after a few months. Therefore, a Japanese traditional curing technique for bamboo (named *Abura Nuki*) was adapted. In this method, a charcoal fire or gas burner is used to extract water, oil and resin from the culms, which is then removed with a rag or wastepaper. A similar process was reported by Richard (2013), using kerosene to improve the removal of the exudate.

In this shortened treatment, a culm with 50–80 mm diameter and 4–5 m length was exposed to the flame of a portable LPG-gas torch (usually used for the application of bituminous membranes) for roughly 5 min. During this process, the culm was constantly rotated about its longitudinal axis, while the distance between the culm and the flame was maintained at about 100 mm, as shown in Fig. 1a. However, we omitted the resin removal phase, letting the exudate dry naturally. The progression of the treatment along the element was monitored by the change in colour of the skin and the amount of resin leakage. After about two weeks of exposure to the sun, the bamboo became shiny, with an agreeable brown tone (Fig. 1b).

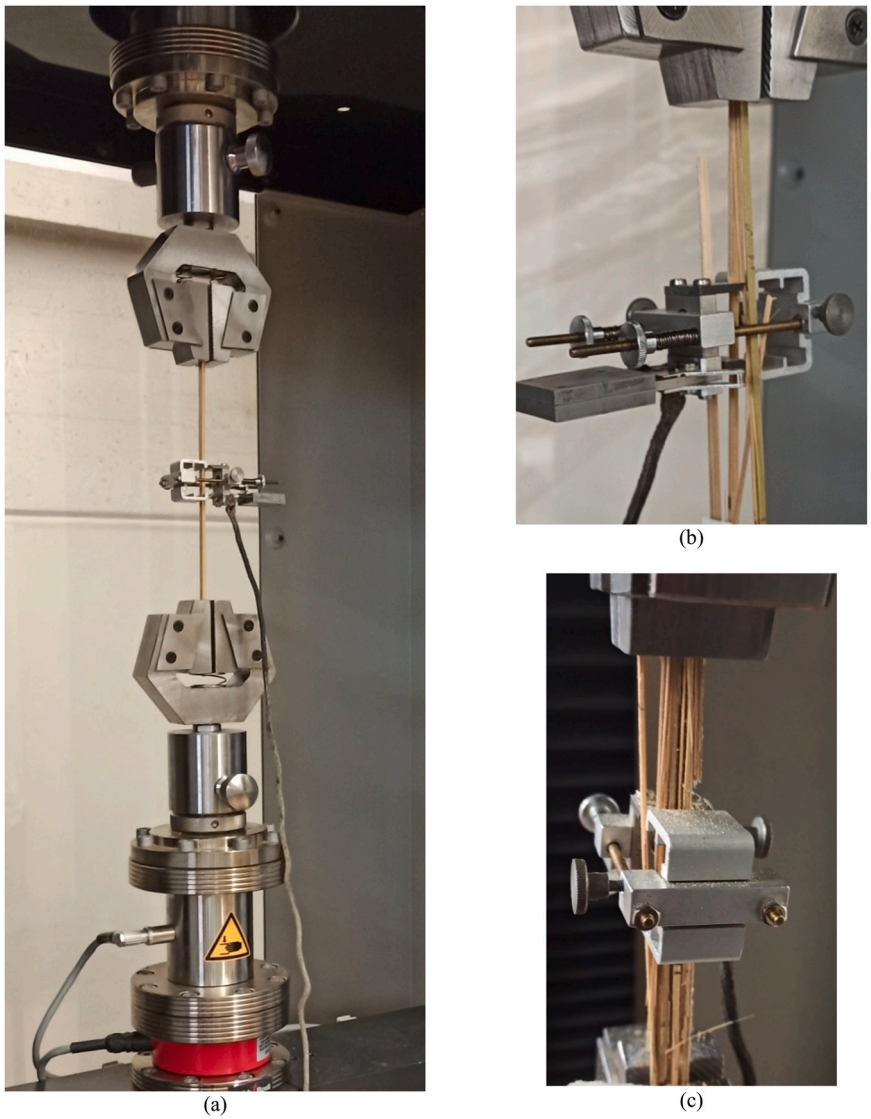

Fig. 2. - Traction setup (a). Failure modes: specimen untreated Ntop1 (b) and specimen treated Tbot11 (c).

Table 2 -
Average values of elastic modulus (longitudinal Young modulus) and strength in tensile tests (in parenthesis the standard deviation and the CV, respectively).

	Not treated			Treated		
	Top	Bottom	All	Top	Bottom	All
$E_{t,o}$ [GPa]	16.6 (3.11; 18.8%)	13.8 (2.25; 16.3%)	15.2 (2.97; 19.5%)	15.1 (1.68; 11.1%)	14.2 (2.30; 16.1%)	14.7 (1.97; 13.4%)
$f_{t,o}$ [MPa]	225.2 (26.8; 11.9%)	199.9 (29.0; 14.5%)	212.6 (31.8; 15.0%)	221.7 (34.0; 15.4%)	192.4 (31.6; 16.4%)	207.1 (34.4; 16.6%)

3. Mechanical characterization of the culms

The mechanical tests and the density and humidity measurements were carried out according to ISO 22157:2019.

3.1. Density and moisture content

The diameters of the culms ranged from 63 to 74 mm. Table 1 shows the mean values, standard deviation and coefficient of variation (CV) of the moisture content (MC) and density of the samples used in tensile tests (the details of each specimen are in Appendix A).

3.2. Tensile test

Following ISO 22157:2019, the tensile specimens were obtained by splitting the culms using a Stanley knife to obtain sticks with rectangular cross-sections. The use of softwood tabs to prevent premature failure at the jaws was bypassed by using an appropriately designed geometry of the grip system, as discussed in detail in Molari (2020, § 3.1 Alternative set up for tension test and Fig. 14). Fig. 2a shows the traction setup, Fig. 2(b)–(c) show the setup and reveal the traction failure mode. The fibres separate into small bundles because of the collapse of the weakest portion of them, with the failure mode being indistinguishable between untreated and treated specimens. Our

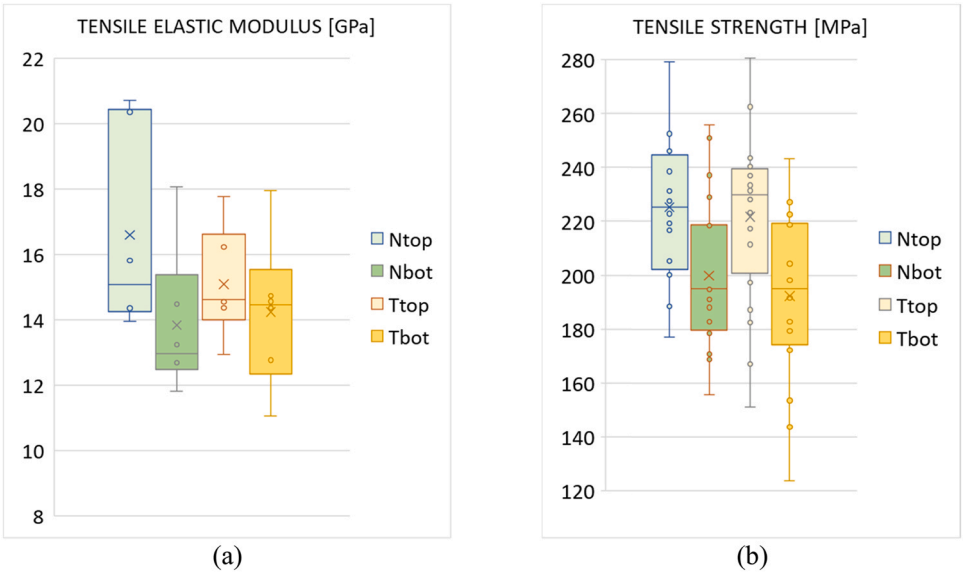

Fig. 3. - Box plot of the tensile test: (a) tensile elastic modulus, (b) tensile strength (the *light* colour shows the *top* specimens, the *dark* colour shows the *bottom* ones).

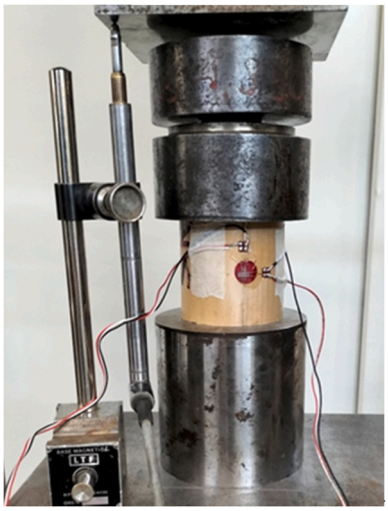

Fig. 4. - Compression setup.

gripping system did not perturb this *natural* failure mechanism, with some fibres remaining intact inside the jaws.

Three specimens were obtained from each of the twelve culms (top + bottom) from the same longitudinal portion of culm, and almost equally distributed around the cross section of the culm, resulting in 36 samples for the top and 36 for the bottom part. Then, specimens (#1 to #12) were equipped with an HMB DD1 extensometer to derive tensile elastic modulus along the fibres $E_{t,0}$. In compliance with the ISO22157:2019, the tension strength, $f_{t,0}$, and the Young modulus, $E_{t,0}$, were obtained as:

$$f_{t,0} = \frac{F_{t,ult}}{A}$$

$$E_{t,0} = \frac{F_{60} - F_{20}}{A(\varepsilon_{60} - \varepsilon_{20})}$$

where $F_{t,ult}$ is the ultimate value of the tensile load, A is the area of the cross section, F_{20} and F_{60} are the 20% and the 60% of $F_{t,ult}$, respectively, with ε_{20} and ε_{60}their related strains. The results of the Young modulus and the tension strength are reported in Table 2 (see Appendix A for more details).

The small coefficient of variations reveals the robustness of the experimental methodology and the homogeneity of the material investigated. The box plots in Fig. 3 show that the heating treatment did not appreciably alter either the elastic modulus or the tension strength:

- the average (top + bottom) tensile elastic modulus was slightly greater for the untreated culms (always greater for the top part with respect to the bottom one, consistent with the results of published studies).
- the average (top + bottom) tensile strength was slightly greater for the untreated culms (greater for the top one).

However, these differences are relatively minor and can be assumed to be insignificant from a structural point of view.

3.3. Compressive test

As suggested by ISO22157 compression tests were performed on cylindrical samples, with the height equal to the minimum value between the external diameter, D, and 10 δ, where δ is the thickness of the culm wall (Fig. 4). To measure the longitudinal and circumferential strains, 6 mm orthogonal bi-directional electrical strain gauges (FCAB-6–11, Tokyo Sokki Kenkyuojo Co., Ltd.) were applied to the central part of the outer surface of the specimens.

Table 3 -
Average values of elastic modulus (longitudinal Young modulus) and strength in compression tests (in parenthesis the standard deviation and the CV, respectively).

	Not treated			Treated		
	Top	Bottom	All	Top	Bottom	All
$E_{c,0}$ [GPa]	20.4 (2.2; 10.6%)	18.9 (2.1; 11.1%)	19.7 (2.1; 10.7%)	21.3 (2.8; 13.1%)	19.2 (2.2; 11.3%)	20.2 (2.5; 12.3%)
$f_{c,0}$ [MPa]	89.7 (9.1; 10.2%)	80.6 (4.2; 5.2%)	85.2 (8.1; 9.5%)	97.3 (1.5; 1.6%)	87.6 (6.0; 6.8%)	92.5 (6.6; 7.1%)

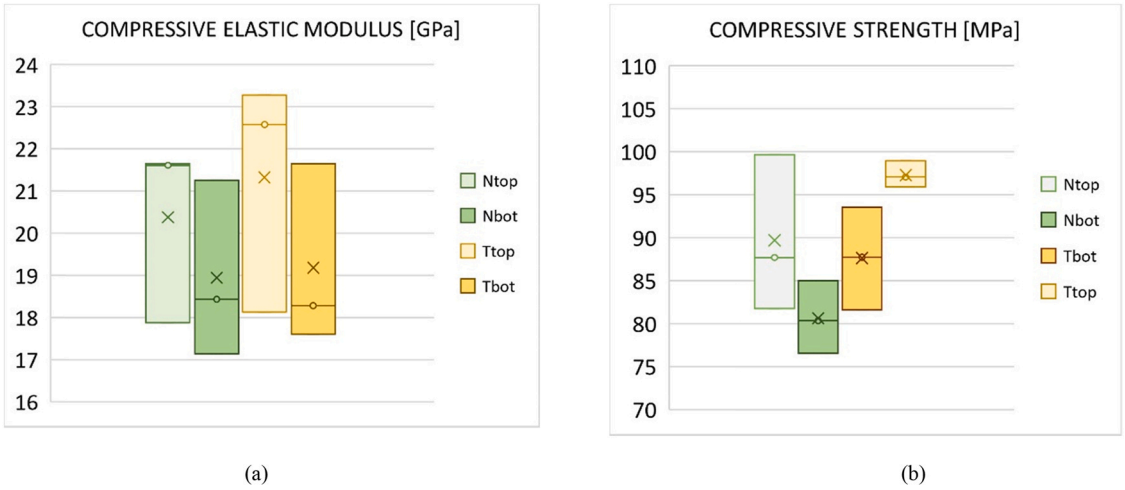

Fig. 5. - Box plot of compression tests: (a) compressive elastic modulus, (b) compressive strength (top specimens shown in a lighter colour, bottom ones in a darker colour).

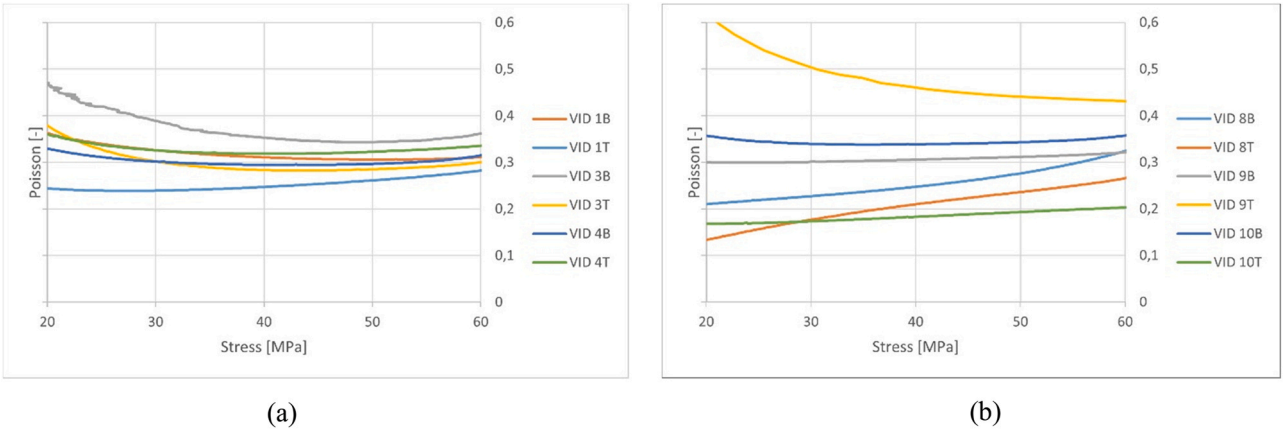

Fig. 6. - Poisson's ratio obtained by the compressive tests: (a) untreated; (b) treated.

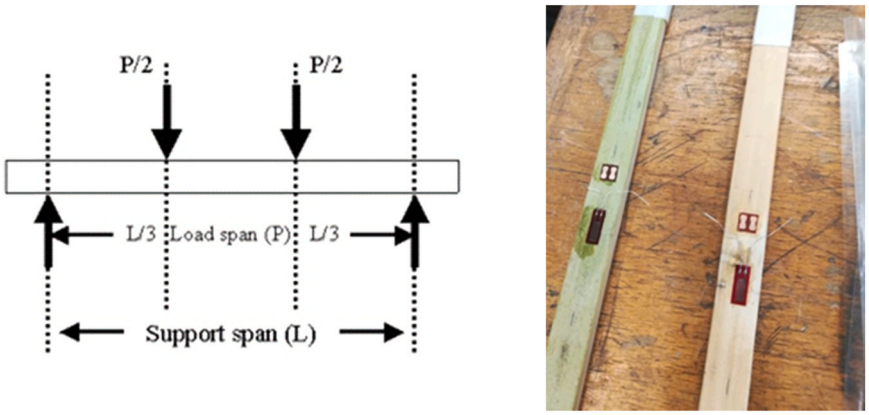

Fig. 7. - Setup of the 4-point bending test and specimens.

The compression strength $f_{c,0}$ was obtained as:

$$f_{c,0} = \frac{F_{c,ult}}{A}$$

where $F_{c,ult}$ is the ultimate load expressed in N and A is the area of the cross section expressed (in mm^2), calculated as a circular crown. The modulus of elasticity in compression parallel to the fibers, $E_{c,0}$, was calculated as the secant between stresses and strains at 20% and 60% of $F_{c,ult}$

$$E_{c,0} = \frac{F_{60} - F_{20}}{A(\varepsilon_{60} - \varepsilon_{20})}$$

where F_{20}, F_{60} is the 20% and the 60% of $F_{c,ult}$, respectively, and ε_{20}, ε_{60} are the related strains. The Young modulus and the strength in compression are reported in Table 3 (see Appendix A for the detailed results).

The box plots in Fig. 5 show that the average (top + bottom) value of the compressive elastic modulus of the treated culms was slightly greater than that of the untreated ones (8%). The compressive strength

Table 4 -
Average values of elastic modulus and strength in bending tests (in parenthesis the standard deviation and the CV, respectively).

	Not treated	Treated
	Bottom	Bottom
$E_{b,o}$ [GPa]	15.5 (3.0; 19.1%)	19.1 (3.7; 19.5%)
$f_{b,o}$ [MPa]	113.3 (18.9; 16.7%)	130.5 (13.3; 10.2%)

was essentially the same in the two sets (with a minimal increase for the treated ones, not statistically significant). Finally, a small increase in the compressive strength of the top part was detected. Once again, these differences were insignificant from a structural point of view.

3.4. Poisson's ratio (in compression tests)

During the compressive tests, a couple of orthogonal strain gauges detect both direct (longitudinal) and indirect (transversal) strains, so that the Poisson's ratio can be immediately derived from the machine data. Fig. 6 shows the relevant results for untreated and treated specimens, respectively, in an intermediate interval of the compressive force.

Independently of the problems of the accuracy and numerical reliability of the Poisson's ratio computation (*cf.* Molari, 2020, Appendix A), these graphs reveal that the treated culms suffered a much greater dispersion than the untreated ones. This outcome was unexpected, given the similar stiffness and strength of the two classes of specimen, and may be partially explained by micro and ultra-microscopic factors, as reported in Section 3.6.

3.5. Bending tests

Several 4-point bending tests were carried out on almost rectangular cross-section specimens cut longitudinally, following the path of the fibres, from a cylindrical portion of the culms (as suggested by UNI 11842:2021). The span between the two supports was L = 180 mm and the loads were equally spaced by L/3 = 60 mm. A 6 mm electrical strain gauge (FLAB-6–11, Tokyo Measuring Instruments Lab.) was applied to the middle of the beam, on the external skin, positioned downwards. The universal material testing machine was a "Woolpert - Amsler" model, with a maximum scale of 1000 N. The tests were carried out in displacement control, with a speed of 7 mm/min, to reach failure in 300 ± 120 s, according to ISO 22157.

The nominal strength was obtained as: Fig. 7.

$$f_{b,0} = \frac{M_{ult} \bullet y}{J}$$

where $M_{ult} = P_{ult} L/2$ is the bending moment related with the maximum load P_{ult}, y is the distance between the external fibre and the neutral axis, J is the inertia moment of the rectangular cross section.

Only samples obtained from the bottom part of the culms were tested: three from untreated and three from treated ones. Table 4 shows the average values and the standard deviations of the Young modulus and bending strength (see Appendix for further details).

The graphs in Fig. 8 reveal that the bending mechanical behaviour is barely influenced by the thermal treatment.

3.6. Microscopic investigations

Two different types of microscopic techniques were employed for each specimen:

- Reflected Polarized Optical Microscopy (RPOM) analyses were performed on thin sections employing a Zeiss Photomicroscope III with polarized light and digitized with an Edmund Optics CMOS-sensor colour camera;
- Environmental Scanning Electron Microscopy (ESEM) analyses were performed on samples without any surface preparation using a Thermofisher Quattro S FE-ESEM field emission electron microscope working at a pressure of 170 Pa and an electron accelerating voltage of 12 kV with a probe current of 0.17 nA, to avoid any sample modification during the analysis.

A small cube was extracted from the transverse cross-section of each culm used for bending test. For the optical observation, the preparation of the bamboo surface required the use of embedding and surface impregnation techniques. Samples were embedded, in a vacuum, with a resin to provide a robust supporting layer and so that they could be cut into small blocks using a wheel saw. The preparation of thin sections involved three steps: (i) grinding the surface (± 1 μm tolerance) using abrasives; (ii) gluing a glass slide onto that surface; (iii) thinning the specimens to 30 μm by means of cutting, lapping and polishing (at least with 0.5 μm grit).

The four micrographs in Fig. 9 (RPOM optical microscope, (a)–(b) inner wall, (c)–(d) outer wall, 10x), show no apparent structural modification of the microstructure of the transverse cross-section of the culm (in both parenchyma and fibre bundle) at optical resolution.

In contrast, using an environmental electron microscope, the ESEM micrographs (Fig. 10, from 150x to 800x) revealed several micro-cracks between the fibre islands of the vascular bundle and the ground parenchyma. These were much more extended and visible in the treated specimens (see Fig. 10b). No modifications were detected near the external skin of the culm wall. Fibre morphology appeared to be unaltered. Similar results are discussed by Akinbade et al. (2019) (§7, Fig. 8), in which some cracks were described as spreading through the fibre bundles. Akinbade et al. (2019) raised the question of whether this

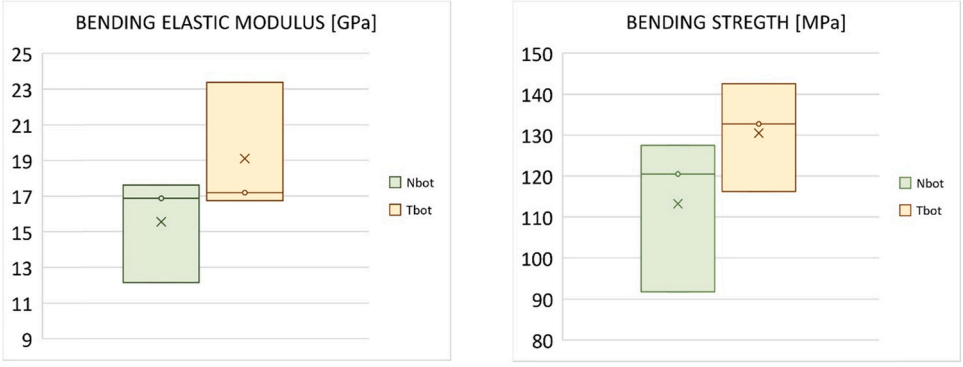

(a) (b)

Fig. 8. - Box plot of bending test: (a) bending elastic modulus, (b) bending strength.

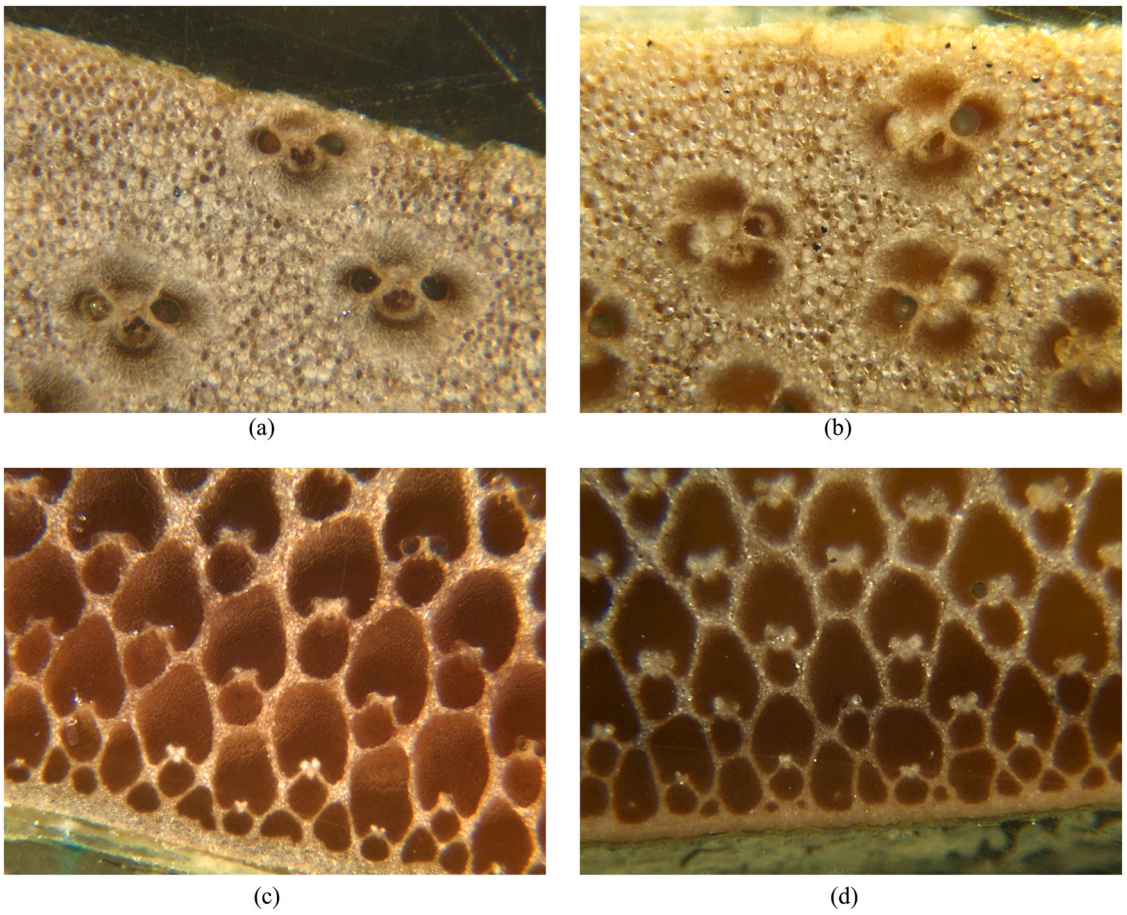

Fig. 9. - RPOM micrographs of the culm cross section (10x). Left: untreated, inner (a) and outer (c) wall. Right: treated, inner (b) and outer (d) wall.

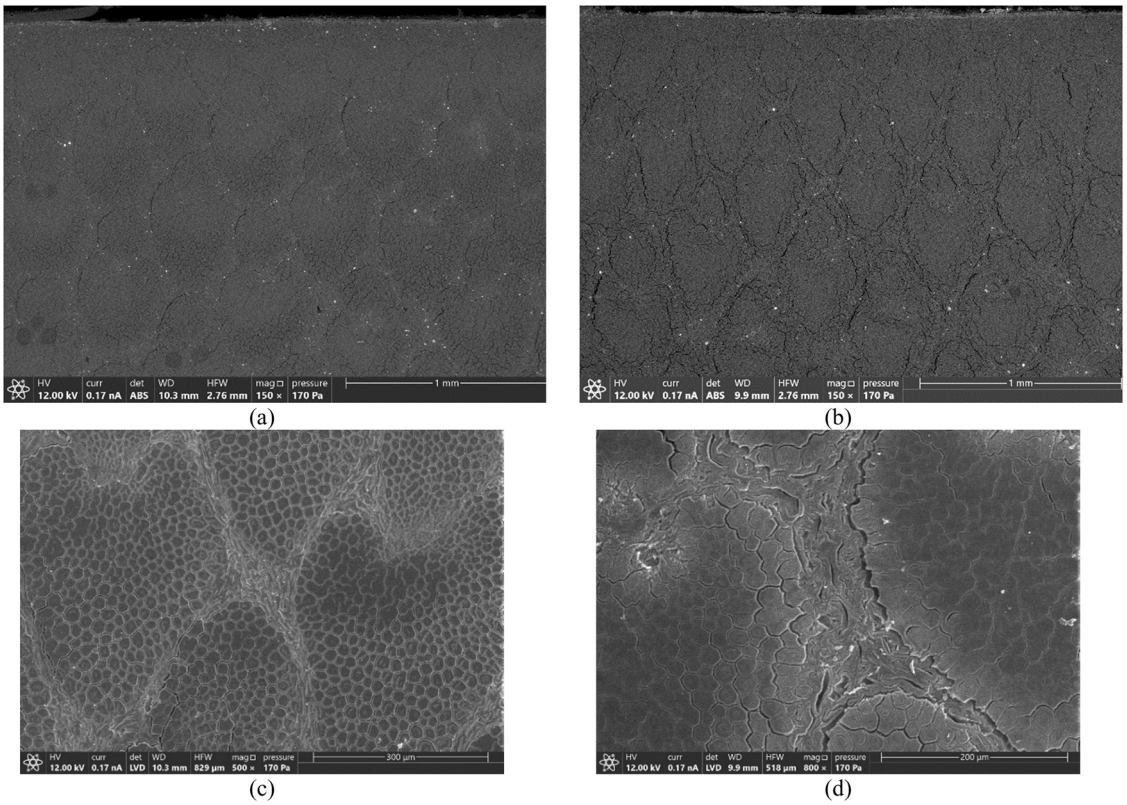

Fig. 10. - ESEM micrographs of the culm cross section. Outer skin and general tissues (150x): (a) untreated, (b) treated. Fibre island and ground parenchyma: (c) untreated (500x), (d) treated (800x). Cracks are evident in the thermally treated bamboo.

deterioration might have been the result of the preparation of the specimen (as well as the seasoning). The same might have been the case in our samples as the machining was quite invasive.

Regardless of their origin, these cracks might explain the transverse response of the material in traction and compression. On the one hand, the longitudinal fibres were not significantly disturbed; on the other hand, the Poisson's ratio was directly affected by the detachment of the fibre bundles from the parenchyma matrix.

4. Discussion

Bamboo materials are more susceptible to degradation then wood, due to both physical and biological agents. Among the non-chemical treatments aimed at reducing the premature deterioration of the culms, relatively short-time heat treatments using a portable LPG-gas torch appear to be very promising. The response of the bamboo is very encouraging as we found no significant reduction in either the elastic modulus or the tensile, compressive and bending strength.

Several samples taken from culms of the bamboo *Phyllostachys viridiglaucescens* were subject to tension (24 top + 24 bottom) and compression (12 top + 12 bottom) tests, in order to compare the response of the treated and untreated culms.

The average (top + bottom) tensile elastic modulus was slightly greater for the untreated culms (always greater for the top than the bottom part, consistent with previously published results). The average (top + bottom) tensile strength was slightly greater for the untreated culms (greater for the top than the bottom). However, these differences were assumed to be insignificant from a structural point of view.

The average value of the compressive elastic modulus of the treated culms was slightly greater than that of the untreated ones (8%). The compressive strength was very similar. A small increase in the compressive strength of the top sections was identified, again consistent with previously published results.

The bending strength was slightly greater for the treated culms as was the elastic modulus. However, the results suggested that the bending behaviour was barely influenced by the thermal treatment.

A microscopic investigation (optical and using an environmental electron microscope ESEM) was undertaken to investigate the possible deterioration of the bamboo microstructure due to the heat treatment. No appreciable damage was detected in the treated material. However, some micro-cracks were observed with the ESEM, and might explain the markedly greater dispersion in the Poisson's ratio for the flame-exposed bamboo.

In conclusion, the proposed heat treatments can be considered a reliable and sustainable protection practice for bamboo culms for two main reasons: a) no appreciable reductions in their mechanical behaviour have been found, and b) the flame treatment may have better human health outcomes than some chemical treatments.

Data Availability

No data was used for the research described in the article.

Declaration of Competing Interest

The authors declare that they have no known competing financial interests or personal relationships that could have appeared to influence the work reported in this paper.

Acknowledgements

The authors wish to thank the editor, Dr. John Innes, for his valuable work, which helped us greatly improve the manuscript, and the Associazione Poliedra, Urbisaglia (MC, Marche), Italy, for its support in providing untreated and treated culms.

Lando Mentrasti would like to thank Carlo Perticarini, Laboratorio Prove Materiali e Strutture, DICEA, UnivPM, for his valuable support in the execution of the tensile test.

Appendix A. Geometrical and physical data

Table A.1
Geometry of culms, moisture content (MC) and density.

	Ntop1	Ntop2	Ntop3	Ntop4	Ntop5	Ntop6	Nbot1	Nbot2	Nbot3	Nbot4	Nbot5	Nbot6
D (mm)	70	70	71	75	73	63	74	70	70	74	74	70
δ (mm)	5.5	6.0	5.5	5.3	6.2	5.0	6.5	7.3	7.3	6.6	8.1	6.1
MC (%)	9.75	9.93	9.53	9.83	9.77	9.43	9.92	9.93	10.03	10.34	9.87	9.70
Density (kg/m^3)	766	713	646	701	713	697	717	631	610	712	602	643
	Ttop7	Ttop8	Ttop9	Ttop10	Ttop11	Top12	Tbot7	Tbot8	Tbot9	Tbot10	Tbot11	Tbot12
D (mm)	76	75	68	76	68	67	74	75	66	74	68	67
δ (mm)	5.9	7.2	5.6	7.0	6.5	5.9	6.8	10.7	6.5	7.2	7.6	7.6
MC (%)	10.17	10.07	9.99	10.01	10.15	10.43	10.14	10.48	10.26	10.25	10.13	10.19
Density (kg/m^3)	709	757	717	734	762	786	740	737	688	759	765	703

Appendix B. Elastic Modulus and Strength

.

Table B.1
Tensions tests: average geometrical properties of specimens.

	Ntop1	Ntop2	Ntop3	Ntop4	Ntop5	Ntop6	Ntop13	Ntop14	Ntop15	Ntop16	Ntop17	Ntop18	Ntop19	Ntop20	Ntop21	Ntop22	Ntop23	Ntop24
b [mm]	3.09	2.91	3.22	3.38	3.36	2.94	2.66	2.17	2.86	3.22	2.92	3.18	2.97	2.78	3.35	3.17	2.71	2.60
t [mm]	5.12	5.70	5.36	5.48	6.08	5.14	5.22	5.35	5.89	5.47	5.59	5.38	5.10	5.02	5.87	5.66	5.16	5.27
	Nbot1	Nbot2	Nbot3	Nbot4	Nbot5	Nbot6	Nbot13	Nbot14	Nbot15	Nbot16	Nbot17	Nbot18	Nbot19	Nbot20	Nbot21	Nbot22	Nbot23	Nbot24
b [mm]	2.84	3.64	3.42	3.44	3.21	3.49	3.17	2.70	3.26	3.91	3.92	3.04	3.48	3.87	3.81	3.78	3.82	3.12
t [mm]	5.90	6.86	6.24	6.34	7.00	6.35	6.07	6.01	6.66	6.93	6.35	6.28	6.42	6.38	7.50	7.10	6.40	6.51
	Ttop7	Ttop8	Ttop9	Ttop10	Ttop11	Ttop12	Ttop25	Ttop26	Ttop27	Ttop28	Ttop29	Ttop30	Ttop31	Ttop32	Ttop33	Ttop34	Ttop35	Ttop36
b [mm]	2.95	3.18	3.03	3.53	2.81	2.68	2.84	2.52	3.25	2.85	2.79	2.86	3.04	3.72	2.85	3.44	2.81	3.05
t [mm]	5.71	6.30	5.80	6.20	6.16	6.14	5.72	5.70	6.42	6.41	5.29	5.53	6.14	6.19	6.41	5.96	5.89	5.79
	Tbot7	Tbot8	Tbot9	Tbot10	Tbot11	Tbot12	Tbot25	Tbot26	Tbot27	Tbot28	Tbot29	Tbot30	Tbot31	Tbot32	Tbot33	Tbot34	Tbot35	Tbot36
b [mm]	3.39	4.62	3.51	3.24	3.52	3.40	2.85	3.19	3.60	3.65	3.24	3.63	3.89	3.81	3.47	3.79	2.82	3.94
t [mm]	6.78	10.64	6.10	6.97	8.21	7.51	6.35	6.72	9.41	9.50	6.25	6.43	7.28	7.28	8.20	8.16	8.25	8.37

Table B.2
Tension tests: elastic modulus along the fibers $E_{t,0}$ [GPa].

Ntop1	Ntop2	Ntop3	Ntop4	Ntop5	Ntop6	Nbot1	Nbot2	Nbot3	Nbot4	Nbot5	Nbot6
20.7	14.4	14.4	14.0	15.8	20.4	11.8	13.2	14.5	18.1	12.7	12.7
Ttop7	Ttop8	Ttop9	Ttop10	Ttop11	Ttop12	Tbot7	Tbot8	Tbot9	Tbot10	Tbot11	Tbot12
12.9	16.2	14.7	14.6	17.8	14.4	14.7	11.1	12.8	14.4	14.6	17.9

Table B.3
Tension tests: tension strength along the fibers $f_{t,0}$ [MPa].

Ntop1	Ntop2	Ntop3	Ntop4	Ntop5	Ntop6	Ntop13	Ntop14	Ntop15	Ntop16	Ntop17	Ntop18	Ntop19	Ntop20	Ntop21	Ntop22	Ntop23	Ntop24
246.1	222.8	200.3	177.0	200.2	188.4	252.5	279.2	240.2	254.2	201.2	205.3	219.3	227.7	216.7	253.4	231.3	238.5
Nbot1	Nbot2	Nbot3	Nbot4	Nbot5	Nbot6	Nbot13	Nbot14	Nbot15	Nbot16	Nbot17	Nbot18	Nbot19	Nbot20	Nbot21	Nbot22	Nbot23	Nbot24
237.1	182.9	191.0	228.9	195.9	194.7	250.9	255.9	218.8	218.4	171.1	168.7	195.5	170.8	155.7	188.0	196.1	178.6
Ttop7	Ttop8	Ttop9	Ttop10	Ttop11	Ttop12	Ttop25	Ttop26	Ttop27	Ttop28	Ttop29	Ttop30	Ttop31	Ttop32	Ttop33	Ttop34	Ttop35	Ttop36
167.1	233.4	228.1	182.5	280.7	231.4	187.2	197.3	234.1	236.9	243.5	262.6	211.5	151.1	223.3	262.5	240.4	217.2
Tbot7	Tbot8	Tbot9	Tbot10	Tbot11	Tbot12	Tbot25	Tbot26	Tbot27	Tbot28	Tbot29	Tbot30	Tbot31	Tbot32	Tbot33	Tbot34	Tbot35	Tbot36
182.9	123.7	198.3	222.6	243.3	179.4	219.4	220.5	143.6	172.2	191.6	172.5	204.3	218.8	227.1	184.4	204.9	153.5

Table B.4
Compression tests: geometrical properties of specimens (wall-thickness δ and diameter D are computed following ISO 22157:2019).

	Ntop1	Ntop3	Ntop4	Nbot1	Nbot3	Nbot4	Ttop8	Ttop9	Ttop10	Tbot8	Tbot9	Tbot10
D [mm]	69.4	65.5	69.1	67.2	65.1	65.4	68.8	60.6	70.7	67.7	62.0	64.8
δ[mm]	5.1	5.3	5.6	7.2	7.3	8.2	5.7	5.1	5.7	7.3	7.2	8.3

Table B.5
Compression tests: elastic modulus along the fibers $E_{c,0}$ [GPa].

Ntop1	Ntop3	Ntop4	Nbot1	Nbot3	Nbot4	Ttop8	Ttop9	Ttop10	Tbot8	Tbot9	Tbot10
21.7	17.9	21.6	21.3	18.4	17.1	18.1	23.3	22.6	21.7	17.6	18.3

Table B.6
Compression tests: compressive strength along the fibers $f_{c,0}$ [MPa].

Ntop1	Ntop3	Ntop4	Nbot1	Nbot3	Nbot4	Ttop8	Ttop9	Ttop10	Tbot8	Tbot9	Tbot10
99.7	81.7	87.7	85.0	76.6	80.3	95.9	97.1	98.9	93.5	81.6	87.7

Table B.7
Bending tests: geometrical properties of specimens (width b and thickness t are computed following UNI 11842:2021).

	Nbot1	Nbot3	Nbot4	Tbot8	Tbot9	Tbot10
L [mm]	237.0	237.0	237.0	235.5	237.0	236.0
b [mm]	12.9	13.6	13.1	12.6	12.2	12.7
t [mm]	6.4	6.6	7.1	7.1	6.2	7.8

Table B.8
Bending tests: bending strength $f_{b,0}$ [MPa] and elastic modulus $E_{b,0}$ [GPa].

	Nbot1	Nbot3	Nbot4	Tbot8	Tbot9	Tbot10
P_{ult} [N]	271.1	399.8	466.1	500.1	307.2	571.8
M_{ult} [Nm]	8.1	12.0	14.0	15.0	9.2	17.2
$f_{b,0}$ [MPa]	91.8	120.5	127.5	142.5	116.2	132.7
ε [%]	0.98	1.26	1.49	1.15	1.20	1.47
$E_{b,0}$ [GPa]	12.2	17.6	16.9	23.4	16.7	17.2

References

Akinbade, Y., Harries, K.A., Flower, C.V., Nettleship, I., Papadopoulos, C., Platt, S., 2019. Through-culm wall mechanical behaviour of bamboo. Constr. Build. Mat. 216, 485–495.

Chang, F.C., Chen, K.S., Yang, P.Y., Ko, C.H., 2018. Environmental benefit of utilizing bamboo material based on Life cycle assessment. J. Clean Prod. 204, 60–69. https://doi.org/10.1016/j.jclepro.2018.08.248

Chung, K.F., Yu, W.K., 2002. Mechanical properties of structural bamboo for bamboo scaffolding. Eng. Struct. 24 (4), 429–442. https://doi.org/10.1016/S0141-0296(01)00110-9

Colla, W.A., Beraldo, A.L., Brito, J.O., 2011. Effects of thermal treatment on the physicochemical characteristics of giant bamboo. Cerne 17 (3), 361–367. https://doi.org/10.1590/S0104-77602011000300010

De Flander, K., Rovers, R., 2009. One laminated bamboo-frame house per hectare per year. Constr. Build. Mater. 23, 210–218. https://doi.org/10.1016/j.conbuildmat.2008.01.004

Escamilla, E.Z., Habert, G., 2014. Environmental impacts of bamboo-based construction materials representing global diversity. J. Clean Prod. 69, 117–127. https://doi.org/10.1016/j.jclepro.2014.01.067

Gauss, C., Savastano Jr., H., Harries, K.A., 2019. Use of ISO 22157 mechanical test methods and the characterization of Brazilian. *P. edulis* bamboo. Constr. Build. Mater. 228, 116728. https://doi.org/10.1016/j.conbuildmat.2019.116728

Gauss, C., Kadivar, M., Pereira, R.G.F., Savastano Jr, H., 2021. Assessment of *Dendrocalamus asper* (Schult and Schult f.) (Poaceae) bamboo treated with tannin-boron preservatives. Constr. Build. Mater. 282, 122723. https://doi.org/10.1016/j.conbuildmat.2021.122723

ISO 221572019. Bamboo structures – Determination of physical and mechanical properties of bamboo culms – Test methods. International Organization for Standardization, Geneva.

Kaminski, S., Lawrence, A., Trujillo, D., King, C., 2016a. Structural use of bamboo. Part 2: durability and preservation. The Structural. Engineer. 94 (10), 38–43.

Kaminski, S., Lawrence, A., Trujillo, D., Feltham, I., Lopez, L.F., 2016b. Structural use of bamboo. Part 3: design values. The Structural Engineer. 94 (12), 42–45.

Kaur, P.J., Satya, S., Pant, K.K., Naik, S.N., 2016. Eco-friendly preservation of bamboo species: traditional to modern techniques. Bioresources. 11 (4), 10604–10624.

Kavanagh, P., Roche, J., Brady, N., Lauder, J., 2020. A comparative Life cycle assessment for utilizing Laminated veneer bamboo as a primary structural material in high-rise residential buildings. In: Choudhury, I., Hashmi, S. (Eds.), Encyclopedia of renewable and sustainable materials, vol.1. Elsevier, pp. 93–113. https://doi.org/10.1016/B978-0-12-803581-8.11299-8

Li, Z.Z., Luan, Y., Hu, J.B., Fang, C.H., Liu, L.T., Ma, Y.F., Liu, Y., Fei, B.H., 2022. Bamboo heat treatments and their effects on bamboo properties. Constr. Build. Mater. 331, 127320. https://doi.org/10.1016/j.conbuildmat.2022.127320

Liese, W., 1998. The anatomy of bamboo culms. Technical Report n 18.

Liese, W., Kohl, M., 2015. Bamboo, The Plant and Its Uses. Springer International Publishing, Switzerland.

Manalo, R.D., Acda, M.N., 2009. Effects of hot oil treatment on physical and mechanical properties of three species of Philippine bamboo. J. Trop. For. Sci. 21 (1), 19–24. ⟨https://www.jstor.org/stable/23616558⟩.

Molari, L., Mentrasti, L., Fabiani, M., 2020. Mechanical characterization of five species of Italian bamboo. Structures 24, 59–72. https://doi.org/10.1016/j.istruc.2019.12.022

Richard, M.J., 2013. Assessing the performance of bamboo structural components, PhD thesis, Swanson School of Engineering, University of Pittsburgh.

Silva Brito, F.M., Benigno Paes, J., Da Silva Oliveira, J.T., Chaves Arantes, M.D., Dudecki, L., 2020. Chemical characterization and biological resistance of thermally treated bamboo. Constr. Build. Mater. 262, 120033. https://doi.org/10.1016/j.conbuildmat.2020.120033

UNI 11842:2021. Bambù – Determinazione delle proprietà fisiche e meccaniche dei culmi di bambù. Ente nazionale italiano di unificazione, Roma.

Van der Lugt, P., Van den Dobbelsteen, A.A.J.F., Janssen, J.J.A., 2006. An environmental, economic and practical assessment of bamboo as a building material for supporting structures. Constr. Build. Mater. 20, 648–656. https://doi.org/10.1016/j.conbuildmat.2005.02.023

Xu, M., Cui, Z., Tu, L., Xia, Q., Chen, Z., 2019. The effect of elevated temperatures on the mechanical properties of laminated bamboo. Constr. Build. Mat. 226, 32–43. https://doi.org/10.1016/j.conbuildmat.2019.07.274

Yang, T.H., Lee, C.H., Lee, C.J., Cheng, Y.W., 2016. Effects of different thermal modification media on physical and mechanical properties of moso bamboo. Constr. Build. Mat. 119, 251–259. https://doi.org/10.1016/j.conbuildmat.2016.04.156

Yu, D., Tan, H., Ruan, Y., 2011. A future bamboo-structure residential building prototype in China: life cycle assessment of energy use and carbon emission. Energy Build. 43, 2638–2646. https://doi.org/10.1016/j.enbuild.2011.06.013

Zhang, Y.M., Yu, Y.L., Yu, W.J., 2013. Effect of thermal treatment on the physical and mechanical properties of *Phyllostachys pubescens* bamboo. Eur. J. Wood Prod. 71, 61–67. https://doi.org/10.1007/s00107-012-0643-6

Zhang, Y., Yu, Y., Lu, Y., Yu, W., Wang, S., 2021. Effects of heat treatment on surface physicochemical properties and sorption behavior of bamboo (*Phyllostachys edulis*). Constr. Build. Mater. 282, 122683. https://doi.org/10.1016/j.conbuildmat.2021.122683